*European Journal of Neuroscience, Vol. 19, pp. 2847–2858, 2004* 

# Distinct properties of presynaptic group II and III metabotropic glutamate receptor-mediated inhibition of perforant pathway–CA1 EPSCs

Marco Capogna
Medical Research Council, Anatomical Neuropharmacology Unit, Mansfield Road, Oxford OX1 3TH, UK

*Keywords*: mGluRs, presynaptic receptors, rat, transmembrane signalling

## Abstract

I have compared the effects of group II or III metabotropic glutamate receptor (mGluR) activation on monosynaptic excitatory responses recorded intracellularly from CA1 pyramidal neurons of rat hippocampus and evoked by perforant pathway stimulation *in vitro*. The excitatory postsynaptic currents (EPSCs) were reduced either by the group II mGluR agonist LY354740 (500 nM, 31 ± 6% of control) or by the group III agonist L-AP4 (400 μM, 53 ± 5% of control). Both drugs enhanced EPSC paired-pulse facilitation (range 125–189% of control). These effects were blocked by the broad-spectrum mGluR antagonist LY341495 (1 or 20 μM) which when applied alone did not significantly change the EPSCs elicited at low (0.1–0.2 Hz) or higher (1–100 Hz) frequency of stimulation. Prior reduction of the EPSCs induced by L-AP4 did not occlude the subsequent inhibition elicited by LY354740. The effect of LY354740, but not that of L-AP4, was blocked in the presence of the cAMP analogue Sp-cAMPS (20 μM) and with the $K^+$ channel antagonist α-dendrotoxin (125 nM). In contrast, the effect of L-AP4, but not that of LY354740, was prevented by the calmodulin inhibitor ophiobolin A (25 μM) and with the N-type $Ca^{2+}$ channel antagonist ω-conotoxin-GVIA (1 μM). In the presence of the P/Q type $Ca^{2+}$ channel antagonist ω-agatoxin-IVA (400 nM), the EPSCs were depressed either by LY354740 or by L-AP4. Groups II and III mGluRs are segregated at the presynaptic terminal, and there are distinct differences between the properties of the presynaptic inhibition mediated by these two groups of receptors.

## Introduction

Metabotropic glutamate receptors (mGluRs) are activated by L-glutamate, the major excitatory transmitter in mammalian central nervous system, and induce several effects including presynaptic inhibition of neurotransmitter release (Anwyl, 1999; Cartmell & Schoepp, 2000). Eight subtypes of mGluRs have been identified so far and they are classified into three groups (mGluR I, II and III) according to their amino acid sequence similarities, agonist selectivity, and interactions with transduction mechanism components (Conn & Pin, 1997). Group II (mGluR2/3) and group III (mGluR4, mGluR6, mGluR7 and mGluR8) are usually coupled to the cyclic AMP cascade (Conn & Pin, 1997) and are activated most potently by LY354740 and L-AP4, respectively (Schoepp *et al*., 1999).

The group II and III mGluRs are often found to be associated with presynaptic elements. Group III mGluR is mainly detected at presynaptic active zones of synapses (Shigemoto *et al*., 1996, 1997), whereas group II mGluR has been observed at extrasynaptic sites remote from the active zone in the preterminal portion of axon terminals (Yokoi *et al*., 1996; Lujan *et al*., 1997; Shigemoto *et al*., 1997). Both presynaptic locations are consistent with the modulatory action on neurotransmitter release elicited by specific ligands for group II or III mGluRs (Anwyl, 1999; Cartmell & Schoepp, 2000). The segregation of presynaptic mGluRs suggests that either some effector mechanisms and/or the sources of glutamate stimulating these receptors are distinct from each other (Shigemoto *et al*., 1997).

The perforant pathway terminating at CA1 stratum lacunosum moleculare (LM) of hippocampus is an interesting example of axons displaying both group II and group III mGluRs, often associated with type I synapses (Shigemoto *et al*., 1997). In this area of hippocampus, the immunoreactivity for mGluR2 and mGluR7a has been described as very strong and strong, respectively (Shigemoto *et al*., 1997) and, although not enriched, the presence of mGluR4 has also been reported (Corti *et al*., 2002). In addition, segregation of the two types of receptors at glutamatergic axon terminals in this layer of hippocampus is observed, so that mGluR7a and mGluR4 are detected at active zones, whereas mGluR2 are found at preterminal zones (Shigemoto *et al*., 1997; Corti *et al*., 2002). In contrast, the immunoreactivity for group II mGluR is undetectable in the stratum radiatum and in CA1 pyramidal cell layer (Shigemoto *et al*., 1997; Tamaru *et al*., 2001).

Functional data are consistent with the presynaptic localization of group II mGluRs at perforant pathway–CA1 synapses (Kawakami *et al*., 2003). Excitatory synaptic responses recorded from CA1 pyramidal cells are depressed by a group II mGluR agonist when evoked by perforant pathway but not Schaffer collaterals. Further modulatory actions of perforant pathway–CA1 synapses by group II or III mGluR ligands have been studied with extracellular recording (Kew *et al*., 2001, 2002). However, the mechanisms of action of presynaptic mGluRs at this synapse remain unknown.

I have compared the effects of activation of group II or III mGluRs on monosynaptic responses recorded intracellularly from CA1

*Correspondence*: Dr Marco Capogna, as above.
E-mail: marco.capogna@pharm.ox.ac.uk

*Received 27 January 2004, revised 9 March 2004, accepted 12 March 2004*

doi:10.1111/j.1460-9568.2004.03378.x

pyramidal neurons after perforant pathway stimulation to see whether segregated presynaptic mGluRs differ in their functional properties.

## Materials and methods

### *Slice preparation*

The data presented were obtained from 13- to 22-day-old rats. The animals were deeply anaesthetized using isoflurane and decapitated in accordance with procedures approved by the Home Office in line with The Animals (Scientific Procedures) Act, 1986. After decapitation, the brain was quickly removed and placed into ice-cold artificial cerebrospinal fluid (ACSF) of composition (in mM): NaCl, 130; $NaHCO_3$, 24; KCl, 3.5; $NaH_2PO_4$, 1.25; $CaCl_2$, 2.5; $MgSO_4$, 1.5; glucose, 10; and kynurenic acid, 3; saturated with 95% $O_2$–5% $CO_2$, at pH 7.3–7.4. The hemisected brain was then glued onto the stage of a Vibratome (VT1000S, Leica Microsystems, Nussloch, Germany) and horizontal sections of 320 μm thickness (350–450 μm in six experiments) were cut. Slices containing hippocampus, entorhinal and perirhinal cortices were then stored at room temperature in an incubation chamber containing the above ACSF, but without the kynurenic acid, for at least 1 h. Slices were then transferred to a recording chamber (Luigs & Neumann, Ratingen, Germany) and perfused at room temperature at a rate of 1–2 mL/min with continuously oxygenated ACSF identical to that used in the incubation chamber. Prior to recording a cut was made between the CA3 and CA1 regions of the hippocampus to prevent indirect activation of CA1 by perforant pathway stimulation through CA3 or dentate granule cells (Yeckel & Berger, 1990).

### *Electrophysiology and data analysis*

CA1 pyramidal cells were identified using a microscope (Zeiss Axioscop 2 F/S Plus, Jena, Germany) with a 40× immersion differential interference contrast objective coupled to an infrared camera system (Hamamatsu, Hamamatsu-City, Japan). Patch pipettes were pulled (Sutter Instruments Co., Novato, CA, USA) from borosilicate glass (Harvard Apparatus, Edenbridge, Kent, UK), and were filled either with (in mM): K-gluconate, 126; KCl, 4; ATP-Mg, 4; GTP-$Na_2$, 0.3; $Na_2$-phosphocreatine, 10; and HEPES, 10; or with Cs-methanesulphonate, 126; CsCl, 4; ATP-Mg, 4; GTP-$Na_2$, 0.3; $Na_2$-phosphocreatine, 10; and HEPES, 10; buffered to a pH of 7.3, osmolarity 290 mOsmol. Biocytin was added to 1 mL aliquots of intracellular solution at 0.5% before recording. Data obtained with the two different pipette solutions were similar and therefore were pooled. For example, the mean area of the EPSCs during LY354740 was $32 \pm 9$ and $28 \pm 8$% of the control with K-gluconate- and Cs-methanesulphonate-based solutions, respectively ($P > 0.5$ between the two conditions, *t*-test). The DC resistance of the electrodes was 3–6 MΩ when filled with the pipette solution. Whole-cell patch-clamp recordings were performed with an EPC9/2 amplifier (HEKA Elektronik, Lambrecht, Germany) either in current clamp, to assess the cell's firing pattern, or in voltage-clamp at a holding potential of −70 mV and with a gain of 10 mV/pA, to study evoked synaptic currents. Series resistance and whole-cell capacitance were monitored during the recordings to check for stability of the recording conditions. Single or pairs of extracellular stimulations at a repetition rate of 0.1–2 Hz (rectangular pulse of 0.05–0.1 ms width and 50–500μA intensity) were delivered using a concentric bipolar electrode (25 μM platinum–iridium tip, FHC, Bowdoinham, ME, USA) connected to a constant-current isolation unit (A360, WPI, Sarasota, FL, USA). In a few experiments, a monopolar glass patch pipette filled with ACSF was used to stimulate. Train stimulations (10, 40 and 100 Hz) were delivered by a stimulator–pulse generator (Master 8, A.M.P.I., Jerusalem, Israel). The stimulation electrode was placed in the stratum LM of CA1.

All recordings were low-pass filtered at 2 KHz and acquired on-line using a built-in laboratory interface (ITC-16) controlled by Pulse 8.53 software (HEKA). Analysis of evoked synaptic responses was performed using Pulsefit 8.53 software (HEKA) and IGOR Pro 4.0 software (WaveMetrics, Inc., Lake Oswego, OR, USA). The area of the synaptic response was primarily measured because perforant synapses are located at apical dendrites ≈300 μm from the somatic site of recording, and the electrotonic properties attenuate the peak amplitude much more than the integral of the response (Otmakhova *et al*., 2002). The area was measured as an absolute value of the integral of the synaptic current starting immediately after the stimulus artifact and until the end of the event (zero crossing, the point immediately before the second stimulus artifact in the paired-pulse protocol, or the end of the recorded trace). In some experiments, however, the peak amplitude of the response evoked by single sweep stimulation was also measured. Excitatory postsynaptic currents (EPSCs) evoked by pairs of stimuli, at 50-ms interval, at low frequencies (usually 0.2 Hz, in a few experiments 0.1 Hz) were averaged from 30 or 20 consecutive synaptic currents in both control period and during application of the drug. To quantify the data, the mean area of the last 30 or 20 consecutive EPSCs of control, drug application and washout periods were compared. The paired-pulse ratio (PPR) was calculated by dividing the area of the mean EPSC evoked by the second stimulus (EPSC2) with the area of the mean EPSC evoked by the first stimulus (EPSC1). PPR was also obtained by dividing the peak amplitude of mean EPSC2 with the peak amplitude of mean EPSC1. The two methods gave similar results. The inverse square power of the coefficient of variation (CV) of each EPSC was calculated with the formula $1/CV^2 = M^2/\sigma_r^2$, where M is the mean amplitude and $\sigma_r^2$ is the variance of the EPSCs. The following protocols with train stimulation have been used: (i) 7–10 stimuli at 10 Hz, and (ii) 7–10 stimuli at 40–100 Hz, followed by test stimulations at recovery time intervals from 200 to 400 ms from the onset of the pulse train. The repetition rate for these protocols was 20 s. The area of individual EPSCs was measured during the train and the recovery. The area underlying the synaptic response during 8–10 stimuli at 40–100 Hz was also measured as an absolute value of the integral of the synaptic current starting immediately after the stimulus artifact of the first stimulus and until the zero crossing of the current. The stability of EPSCs was assessed to test for any time-dependent variation of EPSCs evoked at 0.2 Hz. Stability was acceptable if over the recording period the mean area of any 30 responses was within 1 SD of the mean area of the first 30 responses. This was fulfilled by three out of three control recordings (range 30–40 min). When the EPSCs were elicited at different frequencies of stimulation the mean area of 30 consecutive responses at each frequency of stimulation was also measured and compared. In order to exclude data from polysynaptic responses the following criteria were used: low jitter (< 0.5 ms), short latency, and absence of failures to train stimulation. Latency was measured as the time between the stimulus artifact and the onset of the synaptic current. Jitter was calculated as the SD of the sweep-to-sweep variation in latency within each neuron averaged over 25 trials. Spontaneous excitatory postsynaptic currents (sEPSCs) were analysed as previously described (Capogna *et al*., 2003).

### *Histological processing and anatomical evaluation*

Following electrophysiological recording, slices were fixed overnight by immersion in fixative containing 4% paraformaldehyde, 0.05% glutaraldehyde and 0.2% saturated picric acid in 0.1 M phosphate buffer (pH 7.4). Fixed slices were then embedded in gelatin and resectioned at 60 μm thickness. The recorded cells were labelled with avidin-biotinylated HRP complex (Vector Laboratories, Burlingame,

CA, USA) followed by peroxidase reaction using diaminobenzidine (0.05%) as chromogen and 0.01% $H_2O_2$ as substrate. The sections were then dehydrated and permanently mounted on slides. The axonal and dendritic patterns of each neuron were analysed at low (40×) and high (100×) magnification.

### Statistics

Average values of 20 or 30 consecutive EPSCs recorded in different cells during control and drug application were compared using the nonparametric Wilcoxon rank test (two-tailed). When three experimental groups were compared, the nonparametric Friedman test (two-tailed) was used. Student's *t*-tests were used when indicated in the text.

### Chemicals and drugs

All drugs were bath-applied and reached a steady-state concentration in the chamber in <2 min. Experiments with ω-conotoxin-GVIA (ω-CTx-GVIA) and ω-agatoxin-IVA (ω-Aga-IVA) were executed in the presence of cytochrome C (0.1 mg/mL) to saturate nonspecific peptide binding sites. (1S,2S,5R,6S)-(+)-2-aminobicyclo-[3.1.0]hexane-2,6-dicarboxylic acid (LY354740; gift from Eli Lilly & Co., Indianapolis, IN, USA) was stored in frozen aliquots of 1 mM in $dH_2O$. (2S)-2-amino-2-[(1S,2S)-2-carboxycycloprop-1-yl]-3-(xanth-9-yl) propanoic acid (LY341495; Tocris Cookson Ltd, Bristol, UK) was stored in frozen aliquots of 10 mM in DMSO. L-(+)-2-amino-4-phosphonobutyric acid (L-AP4; Tocris), was stored in frozen aliquots of 10 mM in $dH_2O$. The following compounds were obtained from Tocris: D-(–)-2-amino-5-phosphonovaleric acid (D-AP5) (–)-bicuculline methochloride (bicuculline), CGP 55845, 6,7-dinitroquinoxaline-2,3-dione (DNQX) (S)-Adenosine, cyclic-3′,5′- (hydrogenphosphorothioate) triethylammonium (Sp-cAMPS) (R)-Adenosine, cyclic-3′,5′- (hydrogenphosphorothioate) triethylammonium (Rp-cAMPS), 6-imino-3-(4-methoxyphenyl)-1(6H)-pyridazinebutanoic acid (SR95531). The toxins ω-CTx-GVIA and ω-Aga-IVA were purchased from Alomone Laboratories (Jerusalem, Israel); α-dendrotoxin (αDTX) was purchased from Latoxan (Valence, France). All the others chemical and drugs used were obtained from Sigma-Aldrich (Poole, UK).

## Results

### General features

Neurons were recorded under visual control and I–V protocols were performed in whole-cell current-clamp mode to assess the firing pattern of the recorded cells in response to depolarizing rectangular current pulses. All neurons included in this study displayed action potential kinetics and discharge patterns with accomodation typical of CA1 hippocampal pyramidal neurons. A few recorded slices have been histologically processed, and the anatomy of the cells analysed. All biocytin-filled neurons analysed ($n = 8$) were identified as CA1 pyramidal cells (not shown).

The EPSCs have been evoked at −70 mV at 0.2 Hz in the presence of a $GABA_A$ antagonist (5 μM bicuculline or SR95331), to isolate the monosynaptic excitatory component of the synaptic response. The monosynaptic nature of the response was challenged by measuring the latency between the stimulus artifact and the onset of the response and the synaptic jitter. Typically the monosynaptic responses displayed a latency of ≈5 ms (mean 5.1 ± 0.4 ms, $n = 5$) and a jitter <0.4 ms (mean 0.33 ± 0.08 ms, $n = 5$). Paired stimuli were applied with a 50-ms interval. Measures of the average PPR in the control, drug and washout are given in Table 1. All the control values were significantly >1 (one-sample *t*-test, with test value 1, two-tailed) and thus displayed paired-pulse facilitation (PPF).

TABLE 1. EPSC area and PPR in control, during LY354740 or L-AP4 and in the presence of various agents

| Experimental conditions | EPSC area (fC) | *n* | PPR | *n* |
|---|---|---|---|---|
| 500 nM LY354740-mediated effects on EPSCs | | | | |
| Control | 1291 ± 93 | 11 | 1.26 ± 0.05 | 11 |
| + LY354740 | 360 ± 58 | 11* | 2.03 ± 0.21 | 11* |
| Wash | 1127 ± 121 | 10 | 1.28 ± 0.06 | 10 |
| Control | 1123 ± 376 | 6 | 1.27 ± 0.17 | 6 |
| 1 μM LY341495 | 1181 ± 410 | 6 | 1.30 ± 0.16 | 6 |
| + LY354740 | 1137 ± 356 | 6 | 1.43 ± 0.15 | 6 |
| Control | 609 ± 106 | 5 | 1.51 ± 0.11 | 5 |
| 25 μM Ophiobolin A | 582 ± 88 | 5 | 1.54 ± 0.10 | 5 |
| + LY354740 | 197 ± 24 | 5* | 2.41 ± 0.20 | 5* |
| Wash | 571 ± 74 | 5 | 1.36 ± 0.07 | 5 |
| Control | 990 ± 235 | 6 | 1.23 ± 0.07 | 6 |
| 1 μM ω-CTx-GVIA | 621 ± 93 | 6* | 1.44 ± 0.04 | 6* |
| + LY354740 | 162 ± 54 | 6* | 1.78 ± 0.09 | 6* |
| Wash | 477 ± 168 | 4 | 1.27 ± 0.10 | 4 |
| Control | 1160 ± 310 | 6 | 1.27 ± 0.14 | 6 |
| 400 nM ω-Aga-IVA | 513 ± 112 | 6* | 1.83 ± 0.42 | 6* |
| + LY354740 | 126 ± 39 | 6* | 2.85 ± 0.49 | 6* |
| Wash | 578 ± 200 | 5 | 1.64 ± 0.17 | 5 |
| Control | 694 ± 70 | 5 | 1.26 ± 0.03 | 5 |
| 125 nM αDTX | 1235 ± 291 | 5* | 1.00 ± 0.09 | 5* |
| + LY354740 | 1079 ± 208 | 5 | 1.05 ± 0.14 | 5 |
| Wash | 1159 ± 284 | 5 | 1.08 ± 0.07 | 5 |
| Control | 732 ± 236 | 5 | 1.47 ± 0.19 | 5 |
| 20 μM Sp-cAMPS | 1212 ± 288 | 5* | 1.25 ± 0.16 | 5 |
| + LY354740 | 1163 ± 264 | 5 | 1.20 ± 0.12 | 5 |
| Wash | 1132 ± 362 | 5 | 1.34 ± 0.33 | 5 |
| Control | 823 ± 187 | 3 | 1.24 ± 0.09 | 3 |
| 200 μM Rp-cAMPS | 850 ± 120 | 3 | 1.18 ± 0.06 | 3 |
| + LY354740 | 217 ± 13 | 3* | 1.74 ± 0.08 | 3* |
| Wash | 738 ± 128 | 3 | 1.30 ± 0.07 | 3 |
| Rp-cAMPS + Sp-cAMPS | 863 ± 165 | 3 | 1.22 ± 0.05 | 3 |
| + LY354740 | 250 ± 45 | 3* | 1.75 ± 0.08 | 3* |
| Control | 1097 ± 180 | 7 | 1.28 ± 0.05 | 7 |
| 400 μM L-AP4 | 544 ± 86 | 7* | 1.70 ± 0.17 | 7* |
| + LY354740 | 179 ± 33 | 7* | 2.34 ± 0.24 | 7* |
| Wash | 1060 ± 179 | 7 | 1.30 ± 0.05 | 7 |
| 400 μM L-AP4-mediated effects on EPSCs | | | | |
| Control | 977 ± 51 | 9 | 1.28 ± 0.09 | 9 |
| + L-AP4 | 520 ± 63 | 9* | 1.67 ± 0.13 | 9* |
| Wash | 876 ± 84 | 9 | 1.38 ± 0.09 | 9 |
| Control | 1210 ± 205 | 4 | 1.20 ± 0.07 | 4 |
| 20 μM LY341495 | 1228 ± 190 | 4 | 1.21 ± 0.11 | 4 |
| + L-AP4 | 1125 ± 243 | 4 | 1.29 ± 0.15 | 4 |
| Control | 666 ± 64 | 5 | 1.30 ± 0.06 | 5 |
| 25 μM Ophiobolin A | 635 ± 77 | 5 | 1.36 ± 0.11 | 5 |
| + L-AP4 | 599 ± 67 | 5 | 1.41 ± 0.11 | 5 |
| Wash | 636 ± 91 | 5 | 1.40 ± 0.13 | 5 |
| Control | 778 ± 130 | 7 | 1.32 ± 0.10 | 7 |
| 1 μM ω-CTx-GVIA | 499 ± 92 | 7* | 1.85 ± 0.31 | 7* |
| + L-AP4 | 455 ± 102 | 7 | 1.84 ± 0.23 | 7 |
| Wash | 465 ± 84 | 7 | 1.80 ± 0.24 | 7 |
| Control | 1008 ± 158 | 8 | 1.17 ± 0.04 | 8 |
| 400 nM ω-Aga-IVA | 488 ± 48 | 8* | 1.55 ± 0.14 | 8* |
| + L-AP4 | 339 ± 47 | 8* | 1.96 ± 0.21 | 8* |
| Wash | 538 ± 66 | 7 | 1.42 ± 0.09 | 7 |
| Control | 618 ± 145 | 6 | 1.56 ± 0.13 | 6 |
| 125 nM αDTX | 852 ± 180 | 6* | 1.26 ± 0.12 | 6* |
| + L-AP4 | 329 ± 86 | 6* | 1.80 ± 0.11 | 6* |
| Wash | 822 ± 178 | 6 | 1.45 ± 0.09 | 6 |
| Control | 752 ± 119 | 5 | 1.16 ± 0.12 | 5 |
| 20 μM Sp-cAMPS | 1309 ± 226 | 5* | 0.94 ± 0.10 | 5 |
| + L-AP4 | 529 ± 80 | 5* | 1.70 ± 0.33 | 5* |
| Wash | 1109 ± 272 | 5 | 0.98 ± 0.07 | 5 |

Data are presented as mean ± SEM. *$P < 0.05$ with Wilcoxon rank test; *n*, number of cells studied.

### *Pharmacological activation of group II or III mGluRs presynaptically inhibits perforant pathway-evoked EPSCs*

The application of the selective group II mGluR agonist LY354740 or the selective group III mGluR agonist L-AP4 (Schoepp *et al*., 1999) depressed the EPSCs evoked by perforant pathway stimulation recorded in CA1 pyramidal neurons in all neurons tested (Figs 1 and 2 and Tables 1 and 2). A representative plot of the time course of the effect elicited by 500 nM LY354740 applied for 10 min is shown in Fig. 1B. On average, the mean area of the EPSCs during LY354740 was $31 \pm 6\%$ of the control and the PPR was $178 \pm 22\%$ of the control ($P < 0.01$ for both, $n = 11$). LY354740 did not change the holding current of the pyramidal cells clamped at $-70$ mV (the mean difference between the holding current during and before the drug was $0.7 \pm 3.2$ pA, $P > 0.5$, $n = 8$). The application of 20 μM DNQX and 40 μM D-AP5 at the end of the experiments always abolished the EPSCs ($n = 6$, Fig. 1B). The $CV^{-2}$ of the EPSCs was decreased by LY354740 from $64 \pm 7$ to $17 \pm 4$ ($P < 0.005$, $n = 11$), indicating higher variability of evoked responses than in control. Likewise, a plot of $CV^{-2}$ against the mean of EPSCs1 before and during LY354740, both normalized to the corresponding control values, showed values close the identity line (Fig. 1D). Thus, the PPR and $CV^{-2}$ data together with the absence of any postsynaptic changes in the recorded cells strongly suggest a presynaptic locus of action by LY354740.

L-AP4 was also applied for 10 min and tested at two different concentrations, 50 and 400 μM, because it is known in functional assays that this compound has an $EC_{50}$ value $<1$ μM for mGluR4, mGluR6 and mGluR8 subtypes, and $>100$ μM for mGluR7 (Schoepp *et al*., 1999). Both concentrations of L-AP4 significantly inhibited the EPSCs in a reversible manner (Fig. 2). Quantitatively, the mean area of the EPSCs during 50 μM L-AP4 was $69 \pm 3\%$ of the control and the PPR was $125 \pm 3\%$ of the control ($P < 0.05$ for both, $n = 5$). Furthermore, the mean area of the EPSCs during 400 μM L-AP4 was $53 \pm 5\%$ of the control and the PPR was $134 \pm 11\%$ of the control ($P < 0.05$ for both, $n = 9$). The effects induced by 400 μM L-AP4 were significantly greater ($P < 0.05$, *t*-test) than the effects elicited by 50 μM L-AP4. The drug did not change the holding current of the cells clamped at $-70$ mV (the mean difference between the holding current during and before 400 μM L-AP4 was $2.7 \pm 1.6$ pA, $P > 0.1$, $n = 5$). The $CV^{-2}$ of the EPSCs was significantly reduced by 400 μM L-AP4 from $60 \pm 21$ to $30 \pm 12$ ($P < 0.01$, $n = 9$), and $CV^{-2}$ data against the mean of EPSCs1 before and during L-AP4 displayed values close the identity line (Fig. 2B). Thus, all the data appear to converge on a presynaptic action by L-AP4.

LY341495 is an antagonist of mGluRs, with nanomolar potency against group II mGluRs and micromolar potency against group III mGluRs (Kingston *et al*., 1998). The application of 1 μM LY341495 for $\approx 15$ min blocked the inhibition of the EPSCs induced by 500 nM

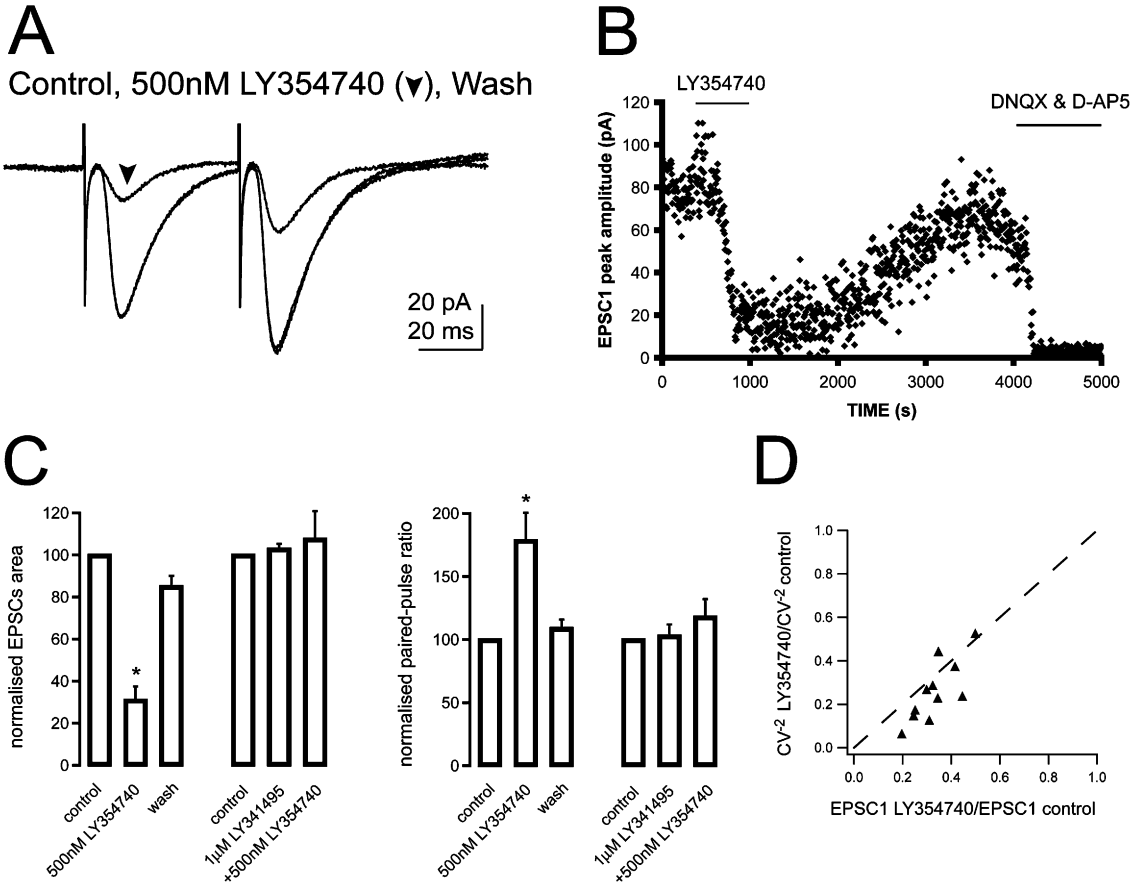


FIG. 1. Activation of group II mGluRs reduced the perforant pathway–CA1 pyramidal cell EPSC. (A) Paired-pulse stimulation before, during and after bath application of the group II mGluR agonist LY354740 (500 nM). The traces shown in this Fig. and in those of Figs 2–7 represent the average of 20 or 30 responses, and a $GABA_A$ antagonist, either SR95331 or bicuculline (5 μM), was present throughout the experiments. (B) Plots of time vs. peak amplitude of individual EPSCs to the first stimulus (EPSC1) for the experiment shown. (C) Normalized pooled data. In the histogram of this Fig. and in those of Figs 2–7, $^*P < 0.05$ compared to the data illustrated by the next left histogram; wash data were not statistically tested. Each mean value is obtained by averaging data from all cells recorded for each protocol (*n* cells is shown in Tables 1 and 2.) (D) Coefficient of variation raised to power $-2$ of EPSC1 plotted against EPSC1 mean peak amplitude, both normalized to the respective control values. The points fall close to the line of unitary slope (dashed line), consistent with a presynaptic effect by LY354740.

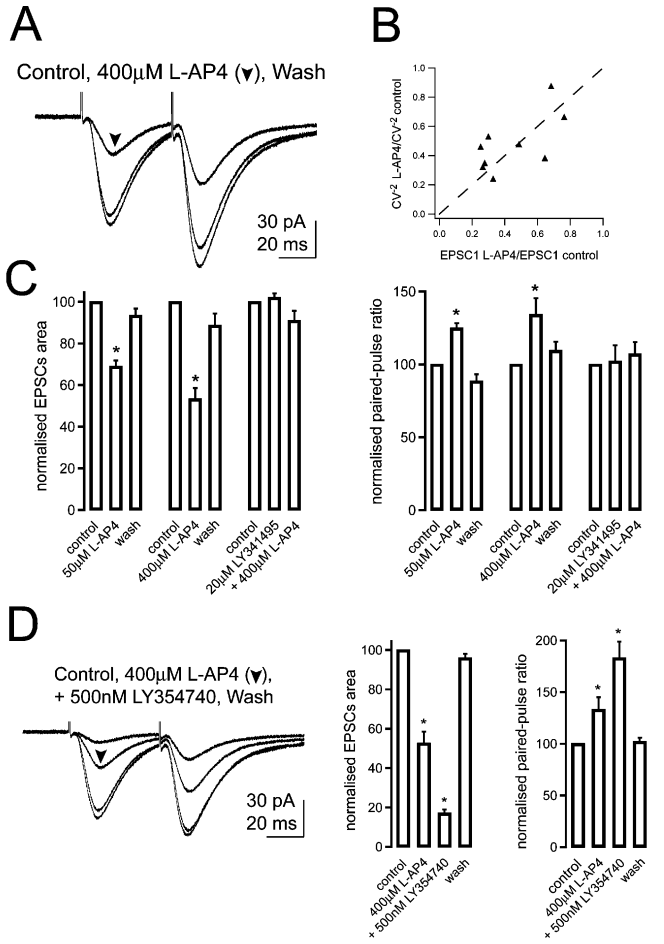


FIG. 2. Activation of group III mGluRs inhibited the perforant pathway–CA1 pyramidal cell EPSC and did not prevent the subsequent effect of LY354740. (A) Superimposed EPSCs evoked by paired-pulse stimulation before, during and after bath application of 400 μM L-AP4. (B) Coefficient of variation raised to power −2 of EPSC1 plotted against EPSC1 mean peak amplitude, both normalized to the respective control values. The points fall close to the line of unitary slope (dashed line), consistent with a presynaptic effect of L-AP4. (C) Normalized pooled data. (D, left) Superimposed EPSCs evoked by paired-pulse stimulation in control, during bath application of 400 μM L-AP4 alone or together with 500 nM LY354740, and after washout of the drugs. (D, right) Normalized pooled data.

LY354740 (mean area of EPSCs and PPR were, respectively, $105 \pm 13$ and $114 \pm 10\%$ of the control; $P > 0.5$ and $P > 0.05$, $n = 6$, Fig. 1C). Likewise, the application of 20 μM LY341495 for ≈ 15 min prevented the inhibition of the EPSCs elicited by 400 μM L-AP4 (mean area of EPSCs and PPR were, respectively, $89 \pm 7$ and $107 \pm 4\%$ of the control; $P > 0.1$ for both, $n = 4$, Fig. 2C). LY341495 did not change the control EPSCs area or PPR (Figs 1C and 2C and Table 1).

Prior application of L-AP4 did not occlude the inhibition induced by LY354740. As shown in Fig. 2D, 400 μM L-AP4 reduced the EPSCs and subsequent application of 500 nM LY354740 further inhibited the EPSCs, which recovered after the washing out of the drugs. On average, in these experiments, the area of the EPSCs and the PPR were $53 \pm 6$ and $133 \pm 12\%$ of the control during 400 μM L-AP4, whereas they were $32 \pm 2$ and $140 \pm 13\%$ of the L-AP4 EPSC and L-AP4 PPR, respectively, during subsequent addition of LY354740 ($P < 0.05$ for all comparisons, $n = 7$). The inhibitions of the EPSCs induced by LY354740 in control conditions and in the presence of

TABLE 2. Percentage inhibition of the EPSCs induced by LY354740 or L-AP4 in control conditions and in the presence of various agents

| Experimental conditions | EPSC LY354740 or L-AP4/control (%) | $n$ |
|---|---|---|
| 500 nM LY354740-mediated effects on EPSCs | | |
| Control + LY354740 | $31 \pm 6.5$ | 11 |
| 1 μM LY341495 + LY354740 | $104.6 \pm 13.3^*$ | 6 |
| 25 μM Ophiobolin A + LY354740 | $35.3 \pm 4.4$ | 5 |
| 1 μM ω-CTx-GVIA + LY354740 | $24.1 \pm 7.4$ | 6 |
| 400 nM ω-Aga-IVA + LY354740 | $20.5 \pm 5.5$ | 6 |
| 125 nM αDTX + LY354740 | $90 \pm 5^*$ | 5 |
| 20 μM Sp-cAMPS + LY354740 | $96.6 \pm 3.2^*$ | 5 |
| 200 μM Rp-cAMPS + LY354740 | $26.8 \pm 4.7$ | 3 |
| 200 μM Rp-cAMPS + 20 μM Sp-cAMPS + LY354740 | $30.2 \pm 5$ | 3 |
| 400 μM L-AP4 + LY354740 | $32.3 \pm 1.7$ | 7 |
| 400 μM L-AP4-mediated effects on EPSCs | | |
| Control + L-AP4 | $53.3 \pm 5.3$ | 9 |
| 20 μM LY341495 + L-AP4 | $89.2 \pm 6.4^*$ | 4 |
| 25 μM Ophiobolin A + L-AP4 | $94.9 \pm 2.6^*$ | 5 |
| 1 μM ω-CTx-GVIA + L-AP4 | $88.6 \pm 8.1^*$ | 7 |
| 400 nM ω-Aga-IVA + L-AP4 | $69.9 \pm 8.1$ | 8 |
| 125 nM αDTX + L-AP4 | $40.4 \pm 5.6$ | 6 |
| 20 μM Sp-cAMPS + L-AP4 | $41.9 \pm 5.8$ | 5 |

Data are presented as mean ± SEM. $^*P < 0.05$ (Student's $t$-test).

400 μM L-AP4 were almost identical ($31 \pm 6.5$ vs. $32.3 \pm 1.7\%$), and the two values were not significantly different ($P > 0.5$, $t$-test).

### *Properties of presynaptic group II or III mGluRs-mediated inhibition of perforant pathway–CA1 EPSC*

#### *Interactions with PKA*

First, the action of the agonists was challenged by Sp-cAMPS, a phosphodiesterase-resistant cAMP analogue, because both group II and III mGluRs are known to be negatively coupled to the cAMP–PKA signal transduction system (Conn & Pin, 1997). The application of 20 μM Sp-cAMPS caused a progressive increase in the area of evoked EPSCs which reached a steady-state size in ≈ 10–15 min from the onset of the application (Fig. 3). The drug also tended to reduce PPR and caused a small inward current in three out of five cells tested (the mean difference between the holding current during and before the drug was $-6.1 \pm 4.2$ pA, $P > 0.1$, $n = 5$). This suggests that Sp-cAMPS elicited mostly presynaptic but also some postsynaptic actions. Subsequent addition of 500 nM LY354740 did not inhibit the EPSCs or change the PPR (Fig. 3A) whereas, in a separate set of experiments, the application of 400 μM L-AP4 always decreased the responses and enhanced the PPR (Fig. 3B). The quantification of the data is shown in Fig. 3C and Tables 1 and 2. There were no attempts to wash out the effect of Sp-cAMPS. Importantly, the PKA inhibitor Rp-cAMPS (200 μM), which blocked the effect of Sp-cAMPS, did not change the inhibition of the EPSCs induced by LY354740 either without or with Sp-cAMPS (Fig. 4). In the presence of Rp-cAMPS, the amount of inhibition elicited by LY354740 was similar to that induced by LY354740 alone (Table 1).

#### *Interactions with calmodulin*

Calmodulin is required to release the βγ subunits of the G-protein heterotrimeric complex from the C-tail of mGluR7a in order to mediate glutamatergic autoinhibition (O'Connor *et al.*, 1999), whereas no molecular data of this type are available for group II mGluRs. Therefore, the mGluR agonists were tested in the presence of ophiobolin A, a calmodulin antagonist. The application of 25 μM ophiobolin

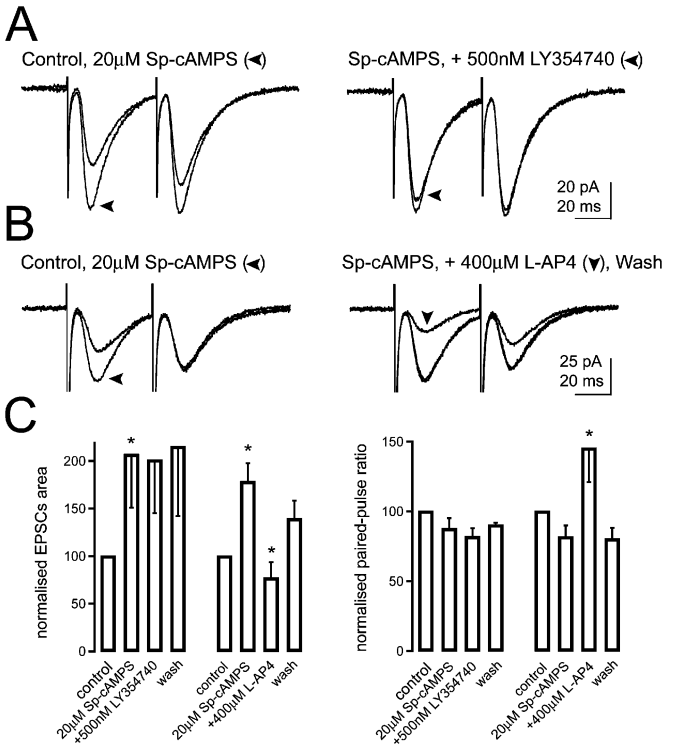


FIG. 3. The PKA activator Sp-cAMPS potentiated EPSCs and blocked the action of LY354740, but not of L-AP4. (A and B) Superimposed EPSCs evoked by paired-pulse stimulation before and during application of 20 μM Sp-cAMPS, and before and during subsequent application of 500 nM LY354740 or 400 μM L-AP4. The response after washout of L-AP4 is also illustrated. (C) Normalized pooled data.

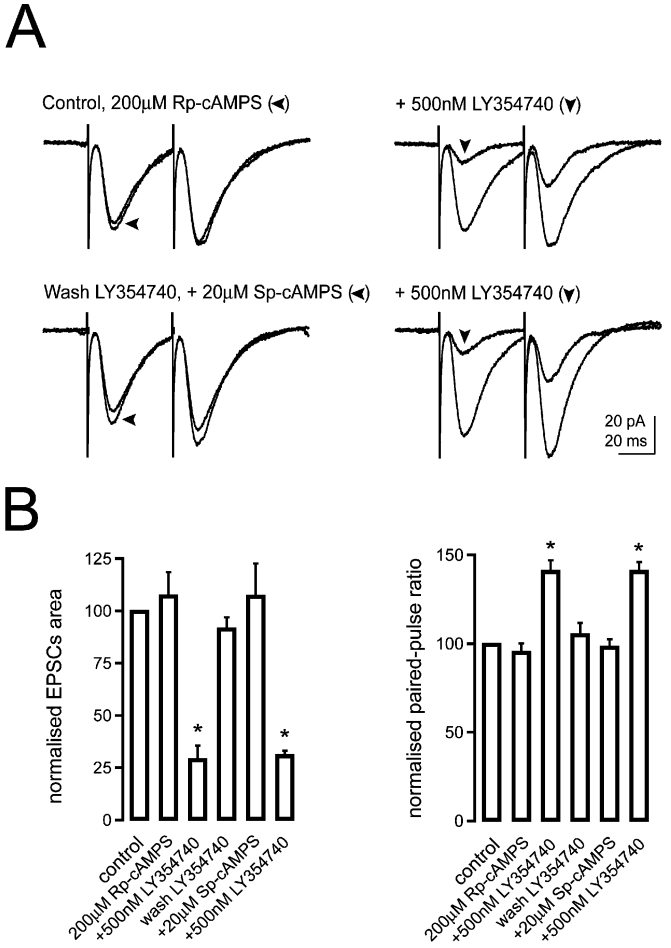


FIG. 4. The PKA inhibitor Rp-cAMPS blocked the effect induced by Sp-cAMPS but not by LY354740. (A) Superimposed EPSCs evoked by paired-pulse stimulation before and during application of 200 μM Rp-cAMPS (upper left) and in the continuous presence of Rp-cAMPS: before and during application of 500 nM LY354740 (upper right), before and during application of 20 μM Sp-cAMPS (lower left) and subsequent addition of 500 nM LY354740 (lower right). (B) Normalized pooled data. Data of these experiments were statistically compared using Student's paired *t*-test.

for 10–15 min did not change the EPSCs (Fig. 5). However, it clearly prevented the inhibition of the EPSCs or the enhancement of PPR induced by 400 μM L-AP4 (Fig. 5A), whereas the effect mediated by 500 nM LY354740 was not blocked (Fig. 5B). The quantification of the data is shown in Fig. 5C and Tables 1 and 2.

### *Interactions with voltage-dependent $Ca^{2+}$ channels*

Voltage-dependent $Ca^{2+}$ channels are likely to be involved in the presynaptic inhibition mediated by mGluRs (Anwyl, 1999). Therefore it was of interest to see whether this mechanism was also operational at the perforant pathway–CA1 synapse. Figure 6A illustrates traces from a representative experiment. The N-type $Ca^{2+}$ channel antagonist ω-CTx-GVIA (1 μM) always produced a partial but irreversible inhibition of the EPSCs which was quite variable in different cells tested (EPSC size range, 42–86% of control). Once a steady-state inhibition by the toxin had been achieved (usually in ≈5–15 min) 500 nM LY354740 was applied and this further reduced the EPSCs in all cells tested. After LY354740 was washed out, the EPSC size recovered and the P/Q type $Ca^{2+}$ channel antagonist ω-Aga-IVA (400 nM) was applied. This antagonist almost completely abolished the residual response, indicating that the simultaneous presence of both $Ca^{2+}$ channel antagonists inhibited the whole pool of presynaptic $Ca^{2+}$ channels (Fig. 6A). In contrast, when 400 μM L-AP4 was tested with the same protocol, this drug only partially and nonsignificantly reduced the residual EPSCs in the presence of ω-CTx-GVIA (Fig. 6B), suggesting that N-type $Ca^{2+}$ channels are required for presynaptic inhibition mediated by group III mGluRs. Furthermore, the reversed protocol was also performed and it was found that 400 nM ω-Aga-IVA did not significantly prevent the inhibition of the EPSCs induced either by 500 nM LY354740 or by 400 μM L-AP4. The quantification of the data is shown in Fig. 6C and in Tables 1 and 2.

### *Interactions with $K^+$ channels*

It has been suggested that $K^+$ channels mediate some of the effects induced by activation of group II or III mGluRs (Anwyl, 1999). α-DTX is a $K^+$ channel antagonist with very interesting features: it blocks several voltage-gated $K^+$ channel subtypes (at least Kv 1.1, 1.2 and 1.6; Mathie *et al*., 1998), and may enhance spontaneous release without changing action potential-evoked intracellular $Ca^{2+}$, in contrast to other $K^+$ channel antagonists active at the synapse such as 4-aminopyridine (Tan & Llano, 1999). Importantly, Kv 1.1 and 1.2 subunits are highly concentrated at axon terminals including the perforant pathway (Monaghan *et al*., 2001). Therefore, the action of the mGluR agonists was tested in the presence of this toxin. αDTX (125 nM) enhanced the area of the evoked EPSCs, reduced the PPR and increased the occurrence of sEPSCs. Thus, this toxin elicited mostly presynaptic actions. In the presence of αDTX, subsequent application of 500 nM LY354740 failed to inhibit the EPSCs (Fig. 7A), whereas 400 μM L-AP4 did cause a clear-cut and reversible inhibition of the EPSCs (Fig. 7B). The quantification of the data is illustrated in Fig. 7C

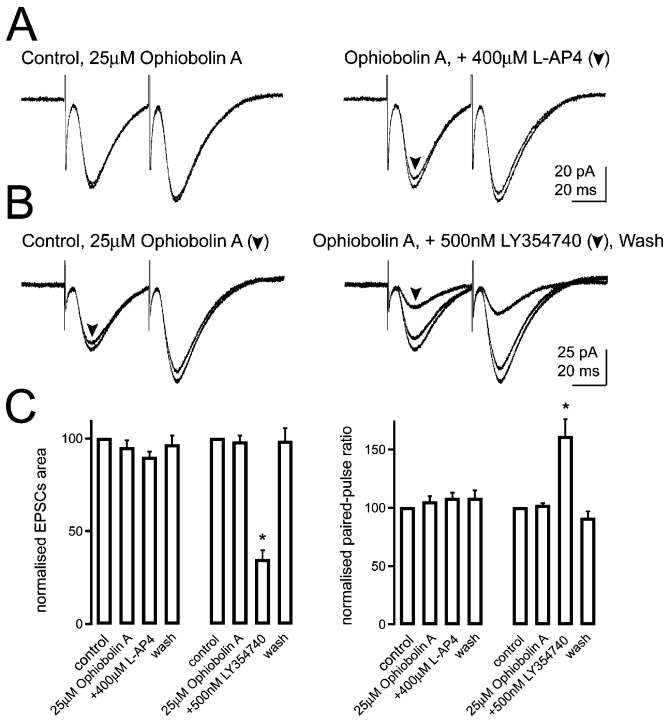


FIG. 5. The calmodulin antagonist ophiobolin A prevents the inhibition of the EPSCs induced by L-AP4 but not by LY354740. (A and B) Superimposed EPSCs evoked by paired-pulse stimulation before and during application of 25 μM ophiobolin and before and during subsequent application of 400 μM L-AP4 or 500 nM LY354740. The response after washout of LY354740 is also shown. (C) Normalized pooled data.

and in Tables 1 and 2. The toxin also caused an increase in the frequency and amplitude of sEPSCs (from $0.87 \pm 0.08$ to $5 \pm 3.5$ Hz and from $13.5 \pm 3.5$ to $19.1 \pm 1.6$ pA, respectively, $n = 4$; not shown). Furthermore, the mGluR antagonist LY341495 (20 μM) did not change the EPSCs increased by αDTX, rendering it unlikely that the increase in release caused by the toxin activated presynaptic mGluRs and saturated or desensitized them, thereby masking the effect of LY354740. On average, the EPSC area after LY341495 was $102 \pm 3\%$ of the αDTX EPSC ($n = 3$; not shown).

### *Does the glutamate released by the perforant pathway activate presynaptic group II or III mGluRs or both?*

The affinity of glutamate for some presynaptic mGluRs is high (Schoepp *et al*., 1999), and therefore it should be possible to detect a feedback inhibition mediated by the activation of presynaptic mGluRs by endogenously released glutamate from afferent fibres, as previously observed at hippocampal mossy fibres (Scanziani *et al*., 1997). Experimentally, I stimulated the perforant pathway with several patterns at high frequency and tested the effect of the broad-spectrum mGluR antagonist LY341495. Because group III are much closer to active zones than group II mGluRs (Shigemoto *et al*., 1997), endogenous release of glutamate should preferentially activate group III mGluR. On the other hand, because the affinity of group II for glutamate is generally higher than for group III mGluR (Schoepp *et al*., 1999), endogenous release of glutamate might preferentially activate group II mGluR. I tested LY341495 at 20 μM, a concentration which was fully effective in blocking the effect of 400 μM L-AP4 (Fig. 2), and which should block both group II and III mGluRs. These experiments were also performed in the presence of the $GABA_A$ antagonist SR95531 (5 μM). First, the application of 20 μM LY341495, up to 15 min, did not change the EPSCs evoked at 0.2, 1 and 2 Hz ($n = 7$, Fig. 8A). On average, in the presence of LY341495, the mean area of the EPSCs was $99 \pm 1\%$ of control at 0.2 Hz stimulation, $98 \pm 2\%$ at 1 Hz and $102 \pm 3\%$ at 2 Hz ($n = 7$). Secondly, control stimulations at 10 Hz, to mimic entorhinal–hippocampal activity at theta frequency, produced a moderate and quite reproducible depression of the response during the train. Usually, this pattern was not markedly altered by LY341495 ($n = 7$, Fig. 8B), although mean increases of 139 and 132% of the size of the EPSCs evoked by the 4th and 5th stimulus were found, essentially caused by the effects seen in two cells. Thirdly, a conditioning train at higher frequency of stimulation, 40 or 100 Hz, was used to mimic entorhinal–hippocampal activity at gamma frequency. In this protocol, test stimuli were also applied at different intervals after the onset of the conditioning train (range 200–400 ms). In the majority of cells, the synaptic current area underlying the train was unaffected by LY341495, as well as the area of the test stimuli elicited at different intervals after the train (Fig. 8C; $n = 8$). An increase of 180 and 190% in the area of the test EPSC after 250 and 300 ms from the onset of the train, respectively, was observed in two different cells, but not in the EPSCs occurring elsewhere after LY341495 application. On average, the mean area underlying the conditioning train stimulation at 100 Hz before and after LY341495 was $4315 \pm 777$ fC and $4302 \pm 821$ fC ($n = 8$), and the mean area underlying the conditioning train stimulation at 40 Hz before and after LY341495 was $22879 \pm 1897$ fC and $23361 \pm 2092$ fC ($n = 8$). Overall, these results indicate that group II and III mGluRs are not overtly activated by glutamate released by the perforant pathway stimulated with high frequency, at least *in vitro*.

## Discussion

### *Inhibitory actions of presynaptic group II and III mGluRs*

Application of the selective group II mGluR agonist LY354740 (500 nM) or the selective group III mGluR agonist L-AP4 (50 μM or 400 μM) (Schoepp *et al*., 1999) reversibly reduced the EPSCs elicited by perforant pathway stimulation and recorded in CA1 pyramidal neurons. Both effects were blocked by the application of the mGluR antagonist LY341495. Paired stimuli elicited PPF in control, which was significantly enhanced by LY354740 or L-AP4. No changes in the holding current or in other electrophysiological parameters were detected. Moreover, analysis of the CV of the responses clearly showed a significantly higher variability during the application of the agonists than in control, and the changes in the $CV^{-2}$ were well correlated with the changes in the mean EPSCs in each cell. These data, taken together, strongly suggest a presynaptic locus of action by the agonists. The present results are consistent with the data obtained from immunolabelling of presynaptic mGluRs at excitatory synapses in stratum LM of CA1 area, which documented immunoreactivity as very strong for mGluR2, strong for mGluR7a, and present, but weaker, for mGluR4, whereas no immunoreactivity for group II or III mGluRs in postsynaptic CA1 pyramidal cells is seen (Shigemoto *et al*., 1997; Tamaru *et al*., 2001; Corti *et al*., 2002). The presynaptic interpretation of my results is also consistent with recent functional data (Kawakami *et al*., 2003) showing that the group II mGluR agonist L-CCG-1 depresses perforant pathway- but not Schaffer collateral-evoked EPSCs recorded in CA1 pyramidal neurons.

When the two mGluR agonists were applied together the percentage of inhibition of the EPSCs by LY354740 in control and in the presence of L-AP4 was similar. No attempts were made to test whether saturating doses of agonists were used, a very difficult task with intracellular data and beyond the aim of the present work. Therefore,

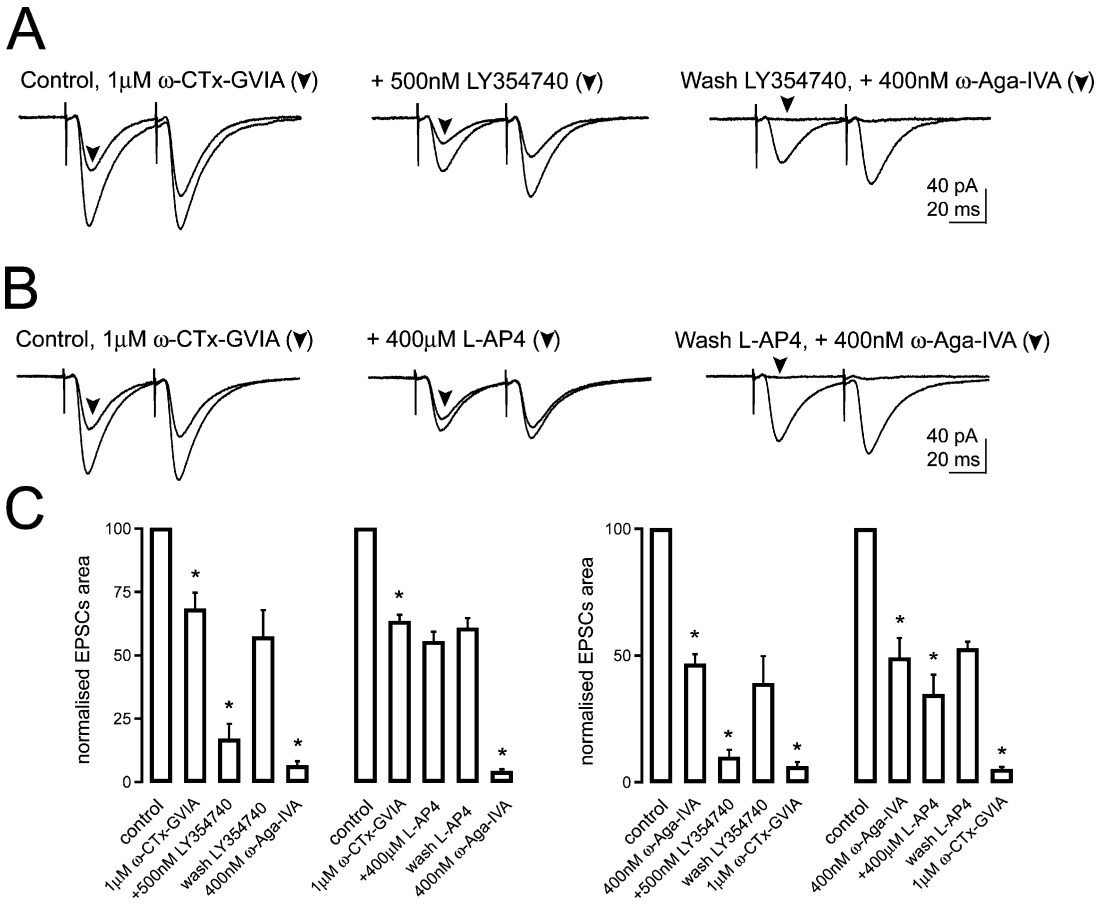


FIG. 6. Actions of $Ca^{2+}$ channel antagonists ω-CTx-GVIA or ω-Aga-IVA on the effects of L-AP4 or LY354740. (A and B) Superimposed controls and EPSCs evoked by paired-pulse stimulation during the application of 1 μM ω-CTx-GVIA, before and during application of 500 nM LY354740 or 400 μM L-AP4, and after washout of the mGluR agonists and application of the P/Q-type $Ca^{2+}$ channel antagonist ω-Aga-IVA (400 nM). (C) Normalized pooled data.

this result is interesting but it does not guarantee that the two groups of mGluRs mediated divergent mechanisms of action.

Which mGluRs are activated in the present experiments? LY354740 is a potent and very selective agonist (up to 1 μM) at mGluR2 and 3 with an $EC_{50}$ of ≈10–50 nM in the rat cortex, hippocampus and striatum, and 10 or 30 nM in cells expressing recombinant mGluR2 or mGluR3, respectively (Schoepp *et al*., 1999). The concentration chosen in the present experiment therefore was 10–50 fold higher than the $EC_{50}$, in order to compensate for the drop in the effective concentration of the drug at synapses within the slice during superfusion. L-AP4 is the most potent and selective agonist for group III mGluRs, including mGluR4, 6, 7 and 8 (Thomsen *et al*., 1992). Unfortunately, it is not selective among individual group III mGluR subtypes (Schoepp *et al*., 1999). I observed a stronger inhibition of the EPSCs with L-AP4 applied at 400 μM than at 50 μM.

A previous extracellular study has described the inhibition elicited by LY354740 or by L-AP4 at perforant inputs to the hippocampal CA1 area (Kew *et al*., 2001). Taking advantage of the stability of the extracellular recordings, this group performed concentration-dependent inhibition curves and found $EC_{50}$ values of 32 nM for LY354740 and 22 μM for L-AP4. On the assumption that differences in the experimental conditions between theirs and the present study would not influence the $EC_{50}$ values, then the concentration of 500 nM I have used for LY354740 would be ≈16-fold higher than the $EC_{50}$ for this compound, and the concentration of 400 μM for L-AP4 would be ≈18-fold higher than the $EC_{50}$ for this compound, at this synapse. Thus, in the present experiments, comparable effective concentrations between the two agonists were used. A difference with the study of Kew *et al*. (2001) is that they did not block the effect of L-AP4 with 3 μM LY341495, whereas I have observed a significant inhibition of the effect of L-AP4 in the presence of 20 μM LY341495. In hippocampal dentate gyrus, agonists for group II and/or III mGluRs clearly depress the excitatory responses between the lateral and/or medial perforant pathway and dentate granule cells (Brown & Reymann, 1995; Ugolini & Bordi, 1995; Macek *et al*., 1996; Kew *et al*., 2001; Kilbride *et al*., 2001). This pathway, however, is quite distinct from that to CA1 pyramidal cells, not only because it targets cells in the dentate gyrus, but also because it originates from layer II stellate cells instead of layer III pyramidal cells of the entorhinal cortex (Steward & Scoville, 1976; Witter, 1993). Presynaptic inhibition induced by pharmacological activation of group II and/or III mGluRs has also been previously observed at other excitatory (Anwyl, 1999; Cartmell & Schoepp, 2000) and also inhibitory synapses (Semyanov & Kullmann, 2000) in the hippocampus.

### *Presynaptic signalling mediated by group II mGluRs*

In the present experiments, PKA activators and αDTX, but not ω-CTx-GVIA or ophiobolin A, blocked the inhibition of the perforant pathway–CA1 EPSC induced by LY354740. In area CA3 or at the medial perforant pathway–dentate granule cell synapses of hippocampus, forskolin or cAMP analogues decrease the ability of group II mGluRs to inhibit excitatory synaptic transmission (Kamiya & Yamamoto,

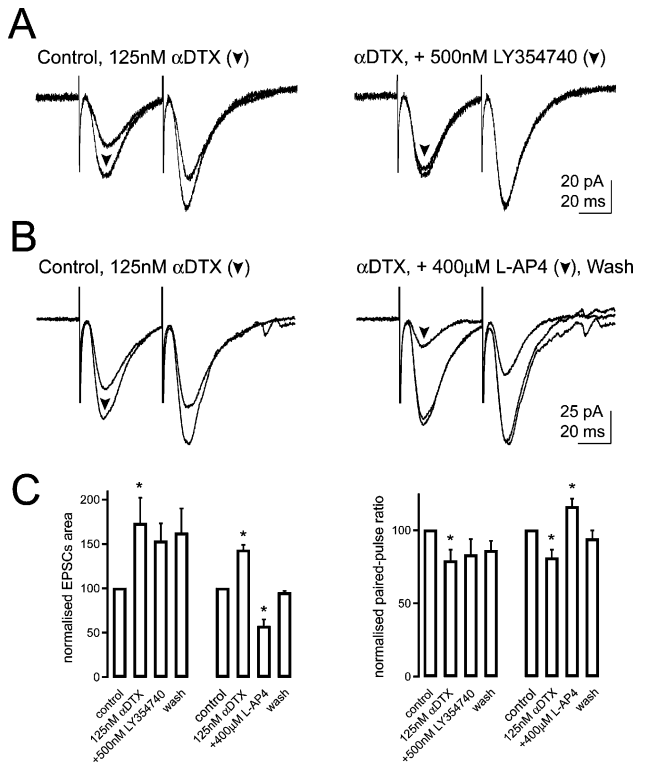


FIG. 7. The $K^+$ channel blocker αDTX inhibited the action of LY354740, but not of L-AP4. (A and B) Superimposed EPSCs evoked by paired-pulse stimulation before and during application of 125 nM αDTX, and during and after subsequent application of 500 nM LY354740 or 400 μM L-AP4. (C) Normalized pooled data.

1997; Maccaferri *et al*., 1998; Schaffhauser *et al*., 2000). A molecular explanation of the cAMP inhibition of group II mGluR function has been provided (Schaffhauser *et al*., 2000). PKA phosphorylates mGluR2 at a single serine residue on the C-terminal tail and the phosphorylation of this site inhibits the coupling of the receptor to GTP-binding proteins. In agreement with Schaffhauser *et al*. (2000), I also found that a PKA inhibitor had no effect on the inhibitory action of LY354740 and blocked the ability of Sp-cAMPS to prevent the LY354740-induced depression. Thus, it is likely that also at the perforant pathway–CA1 excitatory synapse, presynaptic group II mGluRs are functionally uncoupled from GTP-binding proteins by direct PKA phosphorylation.

The present data are consistent with the mechanism that presynaptic group II mGluRs are functionally coupled with α-DTX-sensitive $K^+$ channels. Interestingly, Kv 1.1 and 1.2 subunits sensitive to αDTX have been detected in axon terminals (Wang *et al*., 1993), including entorhinal afferents in rat hippocampus (Monaghan *et al*., 2001), and Kv 1.2 channels are found at preterminal zones of the calyx of Held (Dodson *et al*., 2003). This axonal localization is analogous to the presence of group II mGluRs at preterminal zones of hippocampal axons (Shigemoto *et al*., 1997). Direct patch-clamp recordings of cerebellar basket cell terminals has shown that αDTX-sensitive currents are a significant fraction of the voltage-gated $K^+$ current in this area (Southan & Robertson, 1998). It has also been found that αDTX enhances transmitter release without increasing $Ca^{2+}$ influx into the cerebellar basket cell terminal (Tan & Llano, 1999). It is therefore likely that αDTX-sensitive $K^+$ channels modulate transmitter release from these terminals by changing the action potential threshold and/or determining the occurrence or failure of action potential propagation (Tan & Llano, 1999; Southan & Robertson, 2000). In other nerve terminals, such as hippocampal mossy fibre boutons, αDTX may affect $Ca^{2+}$ influx because the inactivation of αDTX-sensitive channels causes action potential broadening (Geiger & Jonas, 2000). In the present experiments, αDTX enhanced evoked EPSCs and blocked the effect of LY354740, suggesting that group II mGluRs elicited presynaptic inhibition by promoting such αDTX-sensitive axonal mechanism(s). It has been previously shown that the mGluR agonist trans-ACPD presynaptically inhibits EPSCs in visual cortical neurons by a mechanism involving 4-aminopyridine-sensitive $K^+$ channels (Sladeczek *et al*., 1993). The stimulation of group II mGluRs activates G-protein-coupled inwardly rectifying $K^+$ channels in cultured interneurons from cerebellum (Knoflach & Kemp, 1998). In this respect, however, several agonists for presynaptic inhibitory receptors have been found to be still effective when tested at synapses without inwardly rectifying $K^+$ channels (Lüscher *et al*., 1997).

Furthermore, according to the present experiments LY354740 may or may not inhibit both N- and P/Q type $Ca^{2+}$ channels, because neither ω-CTx-GVIA nor ω-Aga-IVA prevented the inhibition of the EPSCs by LY354740. An action through both $Ca^{2+}$ channel types has been suggested for a similar presynaptic effect by a neuropeptide Y agonist at CA3–CA1 excitatory synapses (Qian *et al*., 1997).

Moreover, the calmodulin antagonist ophiobolin A, which by itself did not modify the EPSCs, did not affect the inhibition of the EPSCs elicited by LY354740. It will be interesting to see whether future molecular data will confirm the absence of interactions between calmodulin and group II mGluRs, in contrast to that shown for group III mGluRs (O'Connor *et al*., 1999; El Far *et al*., 2001).

### *Presynaptic signalling mediated by group III mGluRs*

Heterologous expression system data suggest that group III mGluRs inhibit adenylyl cyclase (Pin & Duvoisin, 1995); however, the physiological relevance of this signalling at the nerve terminal remains unclear. Recent results obtained with biochemical and imaging experiments on cerebrocortical nerve terminals provide evidence for a double pathway mediated by mGluR7, either by decreasing the influx of $Ca^{2+}$ through N-type channels or the concentration of cAMP (Millan *et al*., 2002). In their experiments in mGluR7-expressing nerve terminals, L-AP4 inhibits $Ca^{2+}$ entry and glutamate release, and this effect is blocked by ω-CTx-GVIA. Furthermore, L-AP4 reduces glutamate release and cAMP levels enhanced either by forskolin or isoproterenol, but does not reduce basal cAMP concentration (Millan *et al*., 2002). The present electrophysiological observations are consistent with these recent biochemical results, because L-AP4 did not reduce the EPSCs in the presence of ω-CTx-GVIA and inhibited the EPSCs previously enhanced by PKA activation. In addition, αDTX or ω-Aga-IVA did not prevent the action of L-AP4, further suggesting that N-type $Ca^{2+}$ is a major target for group III mGluR modulation. A similar situation exists for the inhibition of EPSCs in the supraoptic nucleus by oxytocin, which is occluded in the presence of ω-CTx-GVIA (Hirasawa *et al*., 2001). However, only P/Q type channels mediate group III mGluR inhibition at the calyx of Held synapse (Takahashi *et al*., 1996). It is interesting that in the presence of ω-Aga-IVA L-AP4 did not cause a stronger inhibition of EPSCs than in control conditions. This can be due to heterogeneity in the expression of presynaptic mGluRs and $Ca^{2+}$ channels, so that in the presence of ω-Aga-IVA a higher proportion of axon terminals with N-type $Ca^{2+}$ channels alone without the coexpression of group III mGluRs are left. Further experiments studying $Ca^{2+}$ influx at individual axon terminals will be necessary to address this issue.

The calmodulin antagonist ophiobolin A blocked the inhibition of the EPSCs elicited by L-AP4 at perforant pathway–CA1 synapses, as

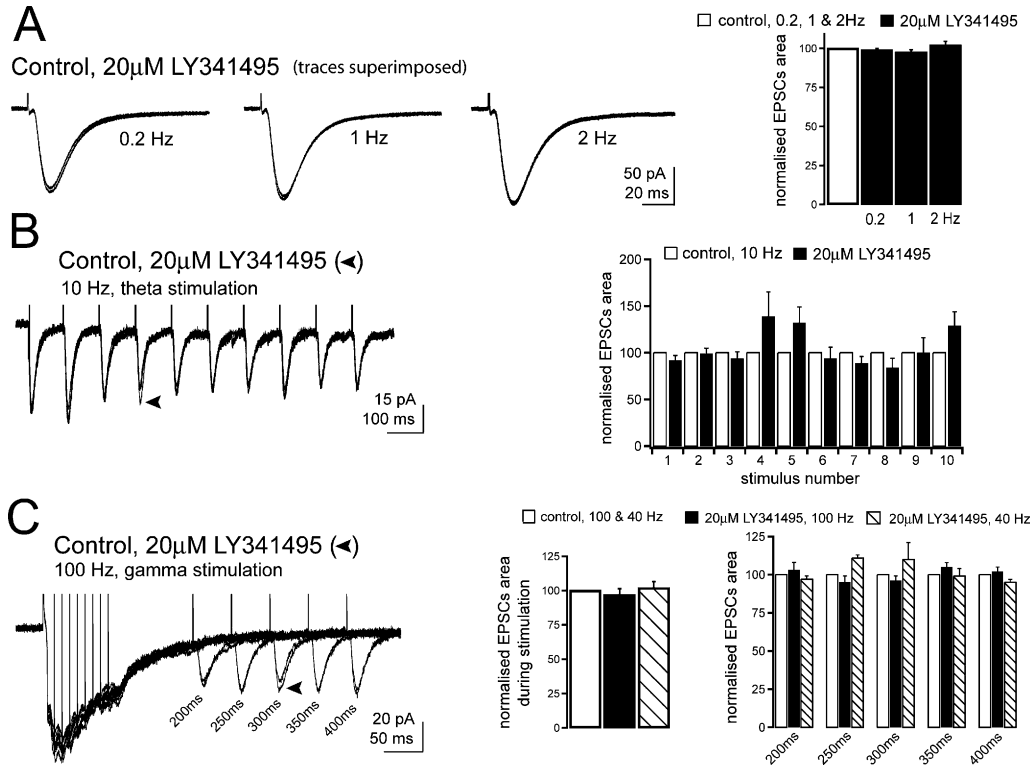


FIG. 8. The groups II and III mGluRs antagonist LY341495 did not change the perforant pathway–CA1 pyramidal cell EPSCs evoked at high frequency of stimulation. (A) Superimposed EPSCs before and during application of 20 μM LY341495 elicited by stimulation at 0.2, 1 or 2 Hz; each trace represents the average of 30 responses. The graph shows normalized EPSCs area before and after LY341495 evoked at 0.2, 1 and 2 Hz ($n = 7$). (B) Superimposed EPSCs before and during application of 20 μM LY341495 induced by train stimulation at 10 Hz; each trace represents the average of seven sweeps and the stimulation artifact has been removed for clarity; the plot illustrates the normalized area of mean EPSCs vs. number of stimuli within the train, in controls and after LY341495 ($n = 7$). (C) Superimposed EPSCs (10 traces) before and during application of 20 μM LY341495 evoked by conditioning train stimulation at 100 Hz followed by test stimulation at 200, 250, 300, 350 and 400 ms after the onset of the train; each trace is the average of seven sweeps; the graph on the left shows the normalized area underlying the conditioning train stimulation at 40 or 100 Hz, and the graph on the right illustrates the normalized area of EPSCs elicited after the onset of the train at various intervals (labels in *x* axis), in controls and after LY341495 ($n = 8$). The $GABA_A$ antagonist SR95531 (5 μM) was present throughout the experiments. All statistical comparisons were non-significant.

previously found at excitatory autaptic currents of hippocampal neurons (O'Connor *et al*., 1999). This result is in agreement with the finding that the binding of calmodulin to the C-terminal portion of mGluR7a promotes G-protein-mediated signalling by displacing the Gβγ subunits from the C-terminal tail of the receptor (O'Connor *et al*., 1999). This mechanism makes the Gβγ subunits available for inhibiting voltage-dependent $Ca^{2+}$ channels, a scenario fully compatible with the present results that the N-type $Ca^{2+}$ channel is involved in the inhibition mediated by L-AP4.

### *Functional consequences of presynaptic mGluRs activation*

Activation of presynaptic mGluRs by endogenous release of glutamate has been examined with high frequency stimulation to produce a sustained release of neurotransmitter before and after the application of LY341495, a competitive broad-spectrum mGluR antagonist. Different patterns of stimulation have been used, including 10, 40 or 100 Hz to mimic theta and gamma activity, which can be recorded *in vivo* in the entorhinal–hippocampal circuitry (Chrobak *et al*., 2000). A recent finding has substantiated the interest in such protocols, because it was observed that $GABA_B$-mediated presynaptic inhibition has a time constant sufficiently rapid to modulate the theta frequency recorded in the hippocampus *in vivo* (Molyneaux & Hasselmo, 2002). However, in the majority of cells tested, I found no difference in the size of the EPSCs before and after LY341495 applied at 20 μM, a concentration which was able to significantly reduce the inhibition by group III mGluRs and which should be saturating for group II mGluRs. The present results are in disagreement with recent data showing that 3 μM LY341495 produces a small but significant increase in the synaptic responses evoked 200 ms after a similar train stimulation of the perforant pathway and recorded extracellularly in CA1 or dentate gyrus of rat or mice (Kew *et al*., 2001, 2002). If one assumes that there is heterogeneity in the activation of presynaptic mGluRs by released glutamate then it is conceivable that one needs to monitor the activity of several synapses to see a significant effect. This possibility is confirmed by the fact that I have observed an increase in the size of the EPSC by LY341495 during theta or after gamma stimulation in a minority of recorded cells. Another important difference is that, in contrast to the present study, the field potentials were recorded by Kew *et al*. (2001, 2002) in the absence of a $GABA_A$ antagonist, and LY341495 may have affected interneuron excitability in their study. Other technical differences, such as the plane used to cut the slices, the depth within the slices of the synapses stimulated by ambient glutamate, and the different recording temperature used, might also account for the different results. Homosynaptic activation of presynaptic mGluRs has previously been detected at hippocampal mossy fibres with intracellular recordings from guinea pig CA3 pyramidal cells (Scanziani *et al*., 1997), as well as heterosynaptic activation of presynaptic mGluRs resulting from spillover of glutamate from nearby releasing sites (Semyanov & Kullmann, 2000). Furthermore, a recent study (Losonczy *et al*., 2003) shows that LY341495 enhances EPSCs

recorded from hippocampal interneurons recorded in stratum oriens–alveus, whereas in the present study LY341495 did not greatly affect EPSCs recorded in CA1 pyramidal cells, suggesting cell-type specific difference in the effect of this compound. The present results agree with the lack of endogenous activation of group III mGluRs during burst stimulation of cortical afferents in the thalamus (Turner & Salt, 1999).

What is the source of glutamate activating presynaptic mGluRs at perforant pathway synapses? As discussed above, the present results do not fully support the idea of homosynaptic activation. It could be that other excitatory fibres, coming from the amygdaloid complex (Pikkarainen *et al*., 1999), the nucleus reuniens (Wouterlood *et al*., 1990) and/or the inferotemporal cortex (Yukie & Iwai, 1988), present in the LM area, heterosynaptically activate the mGluRs at perforant pathway synapses. Due to the considerable difference in the signalling triggered by the group II and III mGluRs described here, and their segregated localization (Shigemoto *et al*., 1997), one is tempted to speculate that the two types of receptors are activated by glutamate released from different axons. However, experimental demonstration of this hypothesis is at present difficult.

### *Conclusion*

The data suggest that group III mGluRs may reduce action potential-evoked transmitter release through a releasing site-delimited action restricted to $Ca^{2+}$ microdomains, locally regulated by calmodulin and by inhibition of $Ca^{2+}$ channels via G-protein βγ subunits. In contrast, the inhibition mediated by group II mGluRs would engage larger domains of the axon terminal plasma membrane and would be modulated by direct receptor phosphorylation by a diffusible agent such as PKA. Thus, it is likely that the segregation of the two groups of mGluRs found at glutamatergic axon terminals (Shigemoto *et al*., 1997; Corti *et al*., 2002) has functional significance.

## Acknowledgements

This work was supported by the Medical Research Council of the UK. I thank Philip Cobden, who showed me how to process the slices for histochemistry, and Mahesh de Alwis, who helped me in preparing solutions and in the histochemical procedures. I also thank Drs David Cope, Francesco Ferraguti, Christopher Price and Massimo Scanziani for their comments on the manuscript, and Eli Lilly & Co., Indianapolis, IN, USA, for supplying LY354740.

## Abbreviations

ACSF, artificial cerebrospinal fluid; αDTX, α-dendrotoxin; bicuculline, (–)-bicuculline methochloride; CV, coefficient of variation; D-AP5, D-(–)-2-amino-5-phosphonovaleric acid; DNQX, 6,7-dinitroquinoxaline-2,3-dione αDTX, α-dendrotoxin; EPSC, excitatory postsynaptic current; L-AP4, L-(+)-2-amino-4-phosphonobutyric acid; LM, lacunosum moleculare; LY341495, (2S)-2-amino-2-[(1S,2S)-2-carboxycycloprop-1-yl]-3-(xanth-9-yl) propanoic acid; LY354740, (1S,2S,5R,6S)-(+)-2-aminobicyclo-[3.1.0]hexane-2,6-dicarboxylic acid; mGluRs, metabotropic glutamate receptors; PPF, paired-pulse facilitation; PPR, paired-pulse ratio; Rp-cAMPS, (R)-Adenosine, cyclic-3′,5′-(hydrogenphosphorothioate) triethylammonium; sEPSCs, spontaneous excitatory postsynaptic currents; Sp-cAMPS, (S)-Adenosine, cyclic-3′,5′- (hydrogenphosphorothioate) triethylammonium; SR95531, 6-imino-3-(4-methoxyphenyl)-1(6H)-pyridazinebutanoic acid; ω-Aga-IVA, ω-Agatoxin-IVA; ω-CTx-GVIA, ω-Conotoxin-GVIA.

## References

Anwyl, R. (1999) Metabotropic glutamate receptors: electrophysiological properties and role in plasticity. *Brain Res. Brain Res. Rev.*, **29**, 83–120.

Brown, R.E. & Reymann, K.G. (1995) Metabotropic glutamate receptor agonists reduce paired-pulse depression in the dentate gyrus of the rat in vitro. *Neurosci. Lett.*, **196**, 17–20.

Capogna, M., Volynski, K.E., Emptage, N.J. & Ushkaryov, Y.A. (2003) The α-latrotoxin mutant $LTX^{N4C}$ enhances spontaneous and evoked transmitter release in CA3 pyramidal neurons. *J. Neurosci.*, **23**, 4044–4053.

Cartmell, J. & Schoepp, D.D. (2000) Regulation of neurotransmitter release by metabotropic glutamate receptors. *J. Neurochem.*, **75**, 889–907.

Chrobak, J.J., Lorincz, A. & Buzsaki, G. (2000) Physiological patterns in the hippocampo-entorhinal cortex system. *Hippocampus*, **10**, 457–465.

Conn, P.J. & Pin, J.P. (1997) Pharmacology and functions of metabotropic glutamate receptors. *Annu. Rev. Pharmacol. Toxicol.*, **37**, 205–237.

Corti, C., Aldegheri, L., Somogyi, P. & Ferraguti, F. (2002) Distribution and synaptic localisation of the metabotropic glutamate receptor 4 (mGluR4) in the rodent CNS. *Neuroscience*, **110**, 403–420.

Dodson, P.D., Billups, B., Rusznák, Z., Szûcs, G., Barker, M.C. & Forsythe, I.D. (2003) Presynaptic rat Kv1.2 channels suppress synaptic terminal hyperexcitability following action potential invasion. *J. Physiol. (Lond.)*, **550**, 27–33.

El Far, O., Bofill-Cardona, E., Airas, J.M., O'Connor, V., Boehm, S., Freissmuth, M., Nanoff, C. & Betz, H. (2001) Mapping of calmodulin and Gbg binding domains within the C-terminal region of the metabotropic glutamate receptor 7A. *J. Biol. Chem.*, **276**, 30662–30669.

Geiger, J.R.P. & Jonas, P. (2000) Dynamic control of presynaptic $Ca^{2+}$ inflow by fast-inactivating $K^+$ channels in hippocampal mossy fiber boutons. *Neuron*, **28**, 927–939.

Hirasawa, M., Kombian, S.B. & Pittman, Q.J. (2001) Oxytocin retrogradely inhibits evoked, but not miniature, EPSCs in the rat supraoptic nucleus: role of N- and P/Q-type calcium channels. *J. Physiol. (Lond.)*, **532**, 595–607.

Kamiya, H. & Yamamoto, C. (1997) Phorbol ester and forskolin suppress the presynaptic inhibitory action of group-II metabotropic glutamate receptor at rat hippocampal mossy fibre synapse. *Neuroscience*, **80**, 89–94.

Kawakami, R., Shinohara, Y., Kato, Y., Sugiyama, H., Shigemoto, R. & Ito, I. (2003) Asymmetrical allocation of NMDA receptor epsilon2 subunits in hippocampal circuitry. *Science*, **300**, 990–994.

Kew, J.N., Ducarre, J.M., Pflimlin, M.C., Mutel, V. & Kemp, J.A. (2001) Activity-dependent presynaptic autoinhibition by group II metabotropic glutamate receptors at the perforant path inputs to the dentate gyrus and CA1. *Neuropharmacology*, **40**, 20–27.

Kew, J.N., Pflimlin, M.C., Kemp, J.A. & Mutel, V. (2002) Differential regulation of synaptic transmission by mGlu2 and mGlu3 at the perforant path inputs to the dentate gyrus and CA1 revealed in $mGlu2^{-/-}$ mice. *Neuropharmacology*, **43**, 215–221.

Kilbride, J., Rush, A.M., Rowan, M.J. & Anwyl, R. (2001) Presynaptic group II mGluR inhibition of short-term depression in the medial perforant path of the dentate gyrus in vitro. *J. Neurophysiol.*, **85**, 2509–2515.

Kingston, A.E., Ornstein, P.L., Wright, R.A., Johnson, B.G., Mayne, N.G., Burnett, J.P., Belagaje, R., Wu, S. & Schoepp, D.D. (1998) LY341495 is a nanomolar potent and selective antagonist of group II metabotropic glutamate receptors. *Neuropharmacology*, **37**, 1–12.

Knoflach, F. & Kemp, J.A. (1998) Metabotropic glutamate group II receptors activate a G protein-coupled inwardly rectifying $K^+$ current in neurones of the rat cerebellum. *J. Physiol. (Lond.)*, **509**, 347–354.

Losonczy, A., Somogyi, P. & Nusser, Z. (2003) Reduction of excitatory responses by persistently active metabotropic glutamate receptors in the hippocampus. *J. Neurophysiol.*, **89**, 1910–1919.

Lujan, R., Roberts, J.D., Shigemoto, R., Ohishi, H. & Somogyi, P. (1997) Differential plasma membrane distribution of metabotropic glutamate receptors mGluR1 alpha, mGluR2 and mGluR5, relative to neurotransmitter release sites. *J. Chem. Neuroanat.*, **13**, 219–241.

Lüscher, C., Jan, L.Y., Stoffel, M., Malenka, R.C. & Nicoll, R.A. (1997) G protein-coupled inwardly rectifying $K^+$ channels (GIRKs) mediate postsynaptic but not presynaptic transmitter actions in hippocampal neurons. *Neuron*, **19**, 687–695.

Maccaferri, G., Toth, K. & McBain, C.J. (1998) Target-specific expression of presynaptic mossy fiber plasticity. *Science*, **279**, 1368–1370.

Macek, T.A., Winder, D.G., Gereau, R., Wt, Ladd, C.O. & Conn, P.J. (1996) Differential involvement of group II and group III mGluRs as autoreceptors at lateral and medial perforant path synapses. *J. Neurophysiol.*, **76**, 3798–3806.

Mathie, A., Wooltorton, J.R.A. & Watkins, C.S. (1998) Voltage-activated potassium channels in mammalian neurons and their block by novel pharmacological agents. *General Pharmacol.*, **30**, 13–24.

Millan, C., Lujan, R., Shigemoto, R. & Sanchez-Prieto, J. (2002) The inhibition of glutamate release by metabotropic glutamate receptor 7 affects both $[Ca^{2+}]c$ and cAMP: evidence for a strong reduction of $Ca^{2+}$ entry in single nerve terminals. *J. Biol. Chem.*, **277**, 14092–14101.

Molyneaux, B.J. & Hasselmo, M.E. (2002) GABA (B) presynaptic inhibition has an in vivo time constant sufficiently rapid to allow modulation at theta frequency. *J. Neurophysiol.*, **87**, 1196–1205.

Monaghan, M.M., Trimmer, J.S. & Rhodes, K.J. (2001) Experimental localization of Kv1 family voltage-gated $K^+$ channel α and β subunits in rat hippocampal formation. *J. Neurosci.*, **21**, 5973–5983.

O'Connor, V.O., El Far, O., Bofill-Cardona, E., Nanoff, C., Freissmuth, M., Karschin, A., Airas, J.M., Betz, H. & Boehm, S. (1999) Calmodulin dependence of presynaptic metabotropic glutamate receptor signaling. *Science*, **286**, 1180–1184.

Otmakhova, N.A., Otmakhov, N. & Lisman, J.E. (2002) Pathway-specific properties of AMPA and NMDA-mediated transmission in CA1 hippocampal pyramidal cells. *J. Neurosci.*, **22**, 1199–1207.

Pikkarainen, M., Ronkko, S., Savander, V., Insausti, R. & Pitkanen, A. (1999) Projections from the lateral, basal, and accessory basal nuclei of the amygdala to the hippocampal formation in rat. *J. Comp. Neurol.*, **403**, 229–260.

Pin, J.P. & Duvoisin, R. (1995) The metabotropic glutamate receptors: structure and functions. *Neuropharmacology*, **34**, 1–26.

Qian, J., Colmers, W.F. & Saggau, P. (1997) Inhibition of synaptic transmission by neuropeptide Y in rat hippocampal area CA1: modulation of presynaptic $Ca^{2+}$ entry. *J. Neurosci.*, **17**, 8169–8177.

Scanziani, M., Salin, P.A., Vogt, K.E., Malenka, R.C. & Nicoll, R.A. (1997) Use-dependent increases in glutamate concentration activate presynaptic metabotropic glutamate receptors. *Nature*, **385**, 630–634.

Schaffhauser, H., Cai, Z., Hubalek, F., Macek, T.A., Pohl, J., Murphy, T.J. & Conn, P.J. (2000) cAMP-dependent protein kinase inhibits mGluR2 coupling to G-proteins by direct receptor phosphorylation. *J. Neurosci.*, **20**, 5663–5670.

Schoepp, D.D., Jane, D.E. & Monn, J.A. (1999) Pharmacological agents acting at subtypes of metabotropic glutamate receptors. *Neuropharmacology*, **38**, 1431–1476.

Semyanov, A. & Kullmann, D.M. (2000) Modulation of GABAergic signaling among interneurons by metabotropic glutamate receptors. *Neuron*, **25**, 663–672.

Shigemoto, R., Kinoshita, A., Wada, E., Nomura, S., Ohishi, H., Takada, M., Flor, P.J., Neki, A., Abe, T., Nakanishi, S. & Mizuno, N. (1997) Differential presynaptic localization of metabotropic glutamate receptor subtypes in the rat hippocampus. *J. Neurosci.*, **17**, 7503–7522.

Shigemoto, R., Kulik, A., Roberts, J.D., Ohishi, H., Nusser, Z., Kaneko, T. & Somogyi, P. (1996) Target-cell-specific concentration of a metabotropic glutamate receptor in the presynaptic active zone. *Nature*, **381**, 523–525.

Sladeczek, F., Momiyama, A. & Takahashi, T. (1993) Presynaptic inhibitory action of a metabotropic glutamate receptor agonist on excitatory transmission in visual cortical neurons. *Proc. R. Soc. Lond.*, **253**, 297–303.

Southan, A.P. & Robertson, B. (1998) Patch clamp recordings from cerebellar basket cell bodies and their presynaptic terminals reveal an asymmetric distribution of voltage-gated potassium channels. *J. Neurosci.*, **18**, 948–955.

Southan, A.P. & Robertson, B. (2000) Electrophysiological characterization of voltage-gated $K^+$ currents in cerebellar basket and Purkinje cells: Kv1 and Kv3 channel subfamilies are present in basket cell nerve terminals. *J. Neurosci.*, **20**, 114–122.

Steward, O. & Scoville, S.A. (1976) Cells of origin of entorhinal cortical afferents to the hippocampus and fascia dentata of the rat. *J. Comp. Neurol.*, **169**, 347–370.

Takahashi, T., Forsythe, I.D., Tsujimoto, T., Barnes-Davies, M. & Onodera, K. (1996) Presynaptic calcium current modulation by a metabotropic glutamate receptor. *Science*, **274**, 594–597.

Tamaru, Y., Nomura, S., Mizuno, N. & Shigemoto, R. (2001) Distribution of metabotropic glutamate receptor mGluR3 in the mouse CNS: differential location relative to pre- and postsynaptic sites. *Neuroscience*, **106**, 481–503.

Tan, Y.P. & Llano, I. (1999) Modulation by $K^+$ channels of action potential-evoked intracellular $Ca^{2+}$ concentration rises in rat cerebellar basket cell axons. *J. Physiol. (Lond.)*, **520**, 65–78.

Thomsen, C., Kristensen, P., Mulvihill, E., Haldeman, B. & Suzdak, P.D. (1992) L-2-amino-4-phosphonobutyrate (L-AP4) is an agonist at the type IV metabotropic glutamate receptor which is negatively coupled to adenylate cyclase. *Eur. J. Pharmacol.*, **227**, 361–362.

Turner, J.P. & Salt, T.E. (1999) Group III metabotropic glutamate receptors control corticothalamic synaptic transmission in the rat thalamus in vitro. *J. Physiol. (Lond.)*, **519**, 481–491.

Ugolini, A. & Bordi, F. (1995) Metabotropic glutamate group II receptors are responsible for the depression of synaptic transmission induced by ACPD in the dentate gyrus. *Eur. J. Pharmacol.*, **294**, 403–410.

Wang, H., Kunkel, D.D., Martin, T.M., Schwartzkroin, P.A. & Tempel, B.L. (1993) Heteromultimeric $K^+$ channels in terminal and juxtaparanodal regions of neurons. *Nature*, **365**, 75–79.

Witter, M.P. (1993) Organization of the entorhinal-hippocampal system: a review of current anatomical data. *Hippocampus*, **3** (Special number), 33–44.

Wouterlood, F.G., Saldana, E. & Witter, M.P. (1990) Projection from the nucleus reuniens thalami to the hippocampal region: light and electron microscopic tracing study in the rat with the anterograde tracer Phaseolus vulgaris-leucoagglutinin. *J. Comp. Neurol.*, **296**, 179–203.

Yeckel, M.F. & Berger, T.W. (1990) Feedforward excitation of the hippocampus by afferents from the entorhinal cortex: redefinition of the role of the trisynaptic pathway. *Proc. Natl. Acad. Sci. USA*, **87**, 5832–5836.

Yokoi, M., Kobayashi, K., Manabe, T., Takahashi, T., Sakaguchi, I., Katsuura, G., Shigemoto, R., Ohishi, H., Nomura, S., Nakamura, K., Nakao, K., Katsuki, M. & Nakanishi, S. (1996) Impairment of hippocampal mossy fiber LTD in mice lacking mGluR2. *Science*, **273**, 645–647.

Yukie, M. & Iwai, E. (1988) Direct projections from the ventral TE area of the inferotemporal cortex to hippocampal field CA1 in the monkey. *Neurosci. Lett.*, **88**, 6–10.